Harmful Algae
July 2022, Volume 116 Pages 102251 (11p.)
https://doi.org/10.1016/j.hal.2022.102251
https://archimer.ifremer.fr/doc/00773/88481/

First subcellular localization of the amnesic shellfish toxin, domoic acid, in bivalve tissues: Deciphering the physiological mechanisms involved in its long-retention in the king scallop *Pecten maximus*

García-Corona Jose Luis [1], Hégaret Helene [4], Deléglise Marc Antoine [1], Marzari Adeline [1], Rodríguez-Jaramillo Carmen [2], Foulon Valentin [3], Fabioux Caroline [1, *]

[1] Institut Universitaire Européen de la Mer, Laboratoire des Sciences de l'Environnement Marin (UMR6539 CNRS/UBO/IFREMER/IRD) Technopôle Brest-Iroise, Plouzané 29280, France
[2] Centro de Investigaciones Biológicas del Noroeste (CIBNOR), Mar Bermejo 195, Col. Playa Palo de Santa Rita, La Paz, B.C.S. 23090, Mexico
[3] Université Bretagne Loire, ENIB, UMR CNRS 6285 LabSTICC, Brest 29238, France
[4] Institut Universitaire Européen de la Mer, Laboratoire des Sciences de l'Environnement Marin (UMR6539 CNRS/UBO/IFREMER/IRD) Technopôle Brest-Iroise, Plouzané 29280, France

* Corresponding author : Caroline Fabioux, email address : cfabioux@univ-brest.fr

Abstract :

Domoic acid (DA), the phycotoxin responsible for amnesic shellfish poisoning (ASP), is an excitatory amino acid naturally produced by at least twenty-eight species of the bloom-forming marine diatoms Pseudo-nitzschia spp. Suspension feeders, such as bivalve mollusks, can accumulate and lengthy retain high amounts of DA in their tissues, threatening human health and leading to extensive-prolonged fishery closures, and severe economic losses. This is particularly problematic for the king scallop Pecten maximus, which retains high burdens of DA from months to years compared to other fast-depurator bivalves. Nonetheless, the physiological and cellular processes responsible for this retention are still unknown. In this work, for the first time, a novel immunohistochemical techniques based on the use of an anti-DA antibody was successfully developed and applied for DA-detection in bivalve tissues at a subcellular level. Our results show that in naturally contaminated P. maximus following a Pseudo-nitzschia australis outbreak, DA is visualized mainly within small membrane-bounded vesicles (1 – 2.5 µm) within the digestive gland cells, identified as autophagosomic structures by means of immune-electron microscopy, as well as in the mucus-producing cells, particularly those from gonad ducts and digestive tract. Trapping of DA in autophagososomes may be a key mechanism in the long retention of DA in scallops. These results and the development of DA-immunodetection are essential to provide a better understanding of the fate of DA, and further characterize DA contamination-decontamination kinetics in marine bivalves, as well as the main mechanisms involved in the long retention of this toxin in P. maximus.

Highlights

► For the first time, domoic acid (DA) was *in situ* detected in the tissues of a bivalve, the king scallop *Pecten maximus.* ► IHC appeared very sensitive allowing visualizing DA into the scallop tissues. ► DA is visualized mainly within autophagosomes from the digestive gland cells. ► Trapping of DA in autophagososomes may be a key mechanism of its long retention in the scallops. ► This work constitute an important step forward in explaining the slow depuration of DA in *P. maximus.*

Keywords : Editor, Jose ? Luis Garcia-Corona, Amnesic shellfish poisoning, Domoic acid, Immunodetection, Toxicokinetics, Scallops, Autophagosomes

1. Introduction

Up to date, fifty-two bloom-forming species of diatoms of the genus *Pseudo-nitzschia* have been identified in all the oceans around the world (Lelong *et al.*, 2012; Bates *et al.*, 2018), and at least twenty-eight of these are capable of synthesizing domoic acid (DA), an extremely dangerous amnesic phycotoxin responsible for amnesic shellfish poisoning (ASP) in humans (Lundholm *et al.*, 2009; Trainer *et al.*, 2012; Zabaglo *et al.*, 2016; Basti *et al.*, 2018). This toxin is a water-soluble amino acid, which acts as a potent neurotransmitter binding to the N-methyl-D-aspartate receptors in neurons of the hippocampus. DA is a structural analog of glutamic acid, proline, and glycine, three neurotransmitters targeting the NMDA-receptors essential to memory and synaptic plasticity, exhibiting respectively a three-fold to 100 fold higher affinity (Zaman *et al.*, 1997; Lefebvre & Robertson, 2010; Zabaglo *et al.*, 2016).

In the last two decades, *Pseudo-nitzschia* blooms have become more intense and frequent worldwide (Lelong *et al.*, 2012; Delegrange *et al.*, 2018), affecting large exploitable populations of suspension-feeding fish and molluscs, which are the main vector of ASP toxin to higher levels of the food chain, since they can accumulate large amounts of DA in their tissues through their filter-feeding activity (Trainer *et al.*, 2012; Hallegraeff, 2017; Basti *et al.*, 2018). Given the toxicity of DA, and as its presence in seafood represents a potential risk for human health, several countries have successfully established monitoring programs in places where *Pseudo-nitzschia* blooms are recurrent and intense (Lelong *et al.*, 2012), and also an international sanitary threshold of 20 mg DA kg^{-1} to regulate the maximum allowable amount of this toxin in bivalves (EFSA, 2009).

The rates of accumulation and depuration of DA in bivalves are species-specific and highly variable (Blanco *et al.*, 2006; Bogan *et al.*, 2007). Therefore, the incidence of toxigenic *Pseudo-nitzschia* blooms on the harvest of natural beds depends on the balance between the kinetics of assimilation and elimination of the toxin (Álvarez *et al.*, 2020; Blanco *et al.*,

2020). In this sense, bivalves have been broadly classified into two wide categories, rapid and slow DA detoxifiers. The former depurate the toxin within days to weeks and includes some species of mussels as *Mytilus galloprovincialis* (Blanco *et al.,* 2002), *M. edulis* (Novaczek *et al.,* 1992; Mafra *et al.,* 2010; Bresnan *et al.,* 2017), and *Perna canalicus* (MacKenzie *et al.,* 1993), oysters such as *Crassostrea virginica* (Mafra *et al.,* 2010) and *C. gigas* (Jones *et al.,* 1995), and pectinids like *Argopecten purpuratus* (Alvarez *et al.,* 2020). The slow depurators can take months to years to depurate the DA. The main examples are some commercially important bivalves like *Pecten maximus* (Blanco *et al.,* 2002; Blanco *et al.,* 2006; Bresnan *et al.,* 2017), *Placopecten magellanicus* (Wohlgeschaffen *et al.,* 1992; Douglas *et al.,* 1997), *Siliqua patula* (Horner *et al.,* 1993), and *Spondylus cruentus* (Ha *et al.,* 2006).

The king scallop *P. maximus* is a high-valuable resource in Europe, and the third most important fishery species in France, with annual catches above 60,000 tons yielding a total of 87 million euros in 2017 (FAO, 2020). Nonetheless, the exploitation of this species is particularly problematic since during blooms of toxigenic *Pseudo-nitzschia* species, scallops can accumulate amounts up to ~3,000 mg DA kg^{-1} in the digestive gland (Blanco *et al.,* 2006), and lengthy retain them, even for years, due to its extremely low depuration rates, from 0.025 to 0.007 d^{-1} (Blanco *et al.,* 2002; Blanco *et al.,* 2006). Considering the slow depuration and the risk for human health, these contamination episodes lead to extensive-prolonged fishery closures, and consequently severe economic losses.

More than 90% of the DA burdens are accumulated in the non-edible tissues of the scallops (Blanco *et al.,* 2006). It has been proposed that DA is mainly in “free-soluble” form in the cytoplasm of the digestive gland cells (Mauriz & Blanco, 2010), and especially in the large digestive (absorptive) cells, responsible of the intracellular digestion of the pinocytized particulate matter using a complex enzymatic equipment in *P. maximus* (Beninger & Le Pennec, 2016). Hence, the digestive cells could have a particular contribution to the high

accumulation of DA in the digestive gland (Blanco *et al.*, 2020). The long retention time of the toxin has been hypothesized to be due to the lack of some efficient membrane transporters in *P. maximus* (Mauriz & Blanco, 2010), or the presence of some high and low-affinity glutamate receptor as the present in the razor clam *Siliqua patula* (Trainer & Bill, 2004). Nevertheless, these hypotheses has not been confirmed yet. Despite the ecological and economic consequences associated with high accumulation of DA in scallops, the mechanisms underlying such a long retention of DA in *P. maximus* are still poorly understood. Hence, the aim of this work was to develop an immunohistochemical method to detect DA at the sub-cellular level in contaminated *P. maximus* tissues and thus decipher the subcellular mechanisms involved in its accumulation and long-retention.

2. Materials and methods

2.1. Biological material and sampling

Twenty adult *Pecten maximus* scallops (9.8 ± 0.1 cm shell length; 171.5 ± 5 g total weight) were collected by dredging from natural beds at three different sites in the west coast of Brittany, France. Six animals were obtained from the Bay of Concarneau (CN) in November 2019 (47° 52' 30.07" N, 3° 55' 20.82" W), and seven more from Camaret-sur-Mer (CM; 48° 26' 33.0096" N, 4° 35' 49.6104" W) in May 2021, after toxigenic *Pseudo-nitzschia* blooms. Additionally, seven scallops were collected from the Bay of Brest (BB) in December 2020 (48° 19' 11" N, 4° 26' 33" W) and used as negative controls since no ASP outbreaks had recently been documented in this area.

Whole soft-bodies were carefully excised from the shells. The organs were then dissected in two groups: a) digestive gland (DG), and b) rest of tissues (RT) which included the gonad, the muscle, the heart, the kidney, the foot, gills and the mantle. As mentioned above, the digestive gland accumulates up to 90% of total domoic acid (DA) burdens (Blanco *et al.*, 2020); for this reason, this organ was first carefully dissected and separated from the RT to avoid any

120 transfer of toxin between organs. Consequently, the DG was separated into three pieces for
121 subsequent histology, toxin quantification, and transmission electron microscopy analysis, as
122 described below. The RT section was used for histology.

123 **2.2. Toxin extraction and quantification by High Performance Liquid Chromatography**
124 **(HPLC)**

125 Since the digestive gland accumulates most of DA, only this tissue was used for DA
126 quantification in this work. For all 20 individuals, DA was extracted from scallop digestive
127 gland following the procedure described by Quilliam *et al.* (1995). Frozen samples (-20 °C)
128 were homogenised from 200 ± 5 mg of tissue in 1 mL of MeOH:MQ water (1:1, v/v) using a
129 Laboratory Mixer Mill MM 400 system (Retsch® Fisher Scientific, Illkirch-Graffenstaden,
130 FR) at 30 Hz/s for 10 min maintaining them in an ice bath. The extract was clarified by
131 centrifugation at 15,000 × g for 10 min at 4 °C (eppendorf 5427 R, Thermo Scientific, West
132 Sussex, UK) and the supernatant was isolated. An aliquot of 200 µL was filtered through a 0.2
133 µm nylon centrifugal filter (VWR International, Radnor, PA, USA) at 10,000 g for 5 min, at 4
134 °C. Since there may be substantial DA degradation in aqueous solutions stored in regular
135 freezer (Thomas *et al.*, 1998), the filtered extracts were stored in amber-glass autosampler
136 vials (Thermo Scientific, Rockwood, TN, USA) at -20 ºC for two days and analysed all at the
137 same time.
138 All fractions obtained were analysed using a Thermo Scientific (Sunnyvale, CA, USA) HPLC
139 System with an UV spectrophotometer Waters 996 PDA-UV detector, using a C18 reverse
140 phase column (5 µm, 250 × 4.6 mm, Phenomenex). The separation was carried out using a
141 mobile phase consisting of eluent A (Distilled water + 0.1 % TFA) and eluent B (ACN + 0.1
142 % TFA) whit gradient conditions from 5 to 20% ACN in 20 min at a flow rate of 1 mL min^{-1},
143 with an injection volume of 20 µL. The column temperature was maintained at 40 °C. A
144 calibration curve was generated by serial dilutions in MeOH:H_2O (1:1, v/v) until

concentrations of 0.2, 0.5, 1.0, 2.0, 4.0 and 8 µg DA mL^{-1} (r = 0.99) of certified DACS-1C DA standards obtained from National Research Council (Halifax, Canada). Thereupon, DA concentration was computed by comparing the absorbance at 242 nm of the chromatographic peaks of the samples with those of the reference solutions once it was checked that the retention time and the absorbance spectrum were the same. The LODs of this HPLC-UV method ranged from 0.2 to 1 mg DA kg^{-1} tissue.

2.3. Histology and Immunohistochemical staining of domoic acid

For all 20 scallops, the piece of digestive gland dedicated to histology (DG) and the rest of the tissues (RT) were separately fixed in Davidson solution for 24 hrs (Kim *et al.*, 2006), and preserved in Ethanol 70 % at 4 °C until processing. Then, tissue samples were dehydrated in ethanol series, cleared in claral, embedded in paraffin (Paraplast Plus, Leica Biosystems, Richmond, IL, USA), thin-sectioned (4 µm), mounted in polysine coated glass-slides (Sigma-Aldrich, St. Louis, MO, USA) and dried overnight at 37 °C (Costa & Costa, 2012), as detailed in Table I. A series of 4 consecutive sections was performed for each samples, which were used for i) immunohistochemical detection of DA (test and negative control), ii) multichromic staining and iii) Hematoxyline/eosin staining.

Sections were deparaffinized and rehydrated in regressive series of ethanol before immunohistochemical staining (Table I). Following preliminary trials, the final procedure employed for immunostaining was performed as described below. An antigen retrieval step was applied in order to break potential methylene bridges formed during formalin-fixation and expose antigenic sites to allow the antibodies epitope to bind. For this, sections were placed in the Universal HIER Antigen Retrieval Reagent (abcam®, Cambridge, UK) diluted in MQ water in a ratio 1:10 (v/v), heated using a pressure cooker until full pressure for 3 min, and subsequently rinsed in washing buffer (TBS 20 mM, NaCl 150 mM, pH 7.6, with 0.025% Triton™ X-100). In order to quench endogenous peroxidase activity, samples were treated

with a Hydrogen Peroxide Blocking Solution (abcam®, Cambridge, UK) at room temperature, and washed in washing buffer.

A polyclonal primary antibody anti-DA (abcam®, Cambridge, UK) was diluted (1: 1,000) in TBS 1× with 1% BSA, applied on slides, and incubated in the dark overnight. Sections were rinsed in washing buffer and then incubated in the dark for 1h with the HRP sharped IgG Goat anti-Rabbit secondary antibody (abcam®, Cambridge, UK) diluted (1:10,000) in TBS 1× with 1% BSA. Immunohistochemistry experimental conditions, as well as antibody optimization-dilutions are detailed in Table II.

Samples were then washed and revealed with diaminobenzidine (DAB+ Chromogen Substrate Kit, abcam®, Cambridge, UK) for 10 min in the dark. Finally, slides were rinsed in washing buffer, counterstained with hematoxylin, and mounted in Faramount Aqueous Medium (Dako®, Carpinteria, CA, USA). The complete version of the suggested immunohistochemical procedure is presented in Table I.

Additionally, a series of slides from the same samples were stained with a multichromic procedure according to Costa & Costa (2012). This technique consists in a combination of Alcian Blue and Periodic Acid–Schiff's for the demonstration of acid mucopolysaccharides and neutral glycoconjugates, in blue and magenta tones, respectively, Hematoxylin blueing for nuclear materials, and Picric Acid to identify proteins in yellow hues.

A last set of sections for both DG and RT was stained with Hematoxylin–Eosin as reference (Kim *et al.*, 2006), and mounted in DPX resin. The slides were examined under a Zeiss Axio Observer Z1 light-microscope. The digestive stages of the diverticula in the DG were classified as holding, absorptive, digestion, advanced digestion, and undergoing breakdown or regeneration, according to Mathers (1976) and Beninger & Le Pennec (2016).

A six-level semi-quantitative scale from 0 (absent) to 2.5 (very high) was established to assess the intensity of the chromogenic anti-DA signal present in the mucus/globose cells of different tissues, the digestive gland, and the small inclusion bodies (IBs) in the digestive cells of the scallops (Table III).

2.4. Transmission electron microscopy and Immunogold labeling

Transmission electron microscopy (TEM) studies were necessary in order to identify the small IBs with chromogenic anti-DA signal within the cells of the digestive gland. For this purposes, three small pieces of DG (~ 1 mm^3) were carefully dissected from some of the non-contaminated scallops collected in the Bay of Brest (n = 5), used as negative controls, and some of the contaminated-scallops from Camaret-sur-Mer (n = 5) with strongest IHC signal in the IBs within the digestive cells. Samples from scallops collected at Concarneau in 2019 were not considered for these analyses since the digestive glands were not processed for TEM purposes.

Samples were pre-fixed in glutaraldehyde 3 % (v/v) with 0.2 M cacodylate buffer (pH 7.4) supplemented with NaCl (21 mg mL^{-1}) for 3 h at 4 °C, rinsed in the same buffer (3 × 5 min), and subsequently post-fixed in 1% (w/v) osmium tetroxide in 0.2 M cacodylate buffer (pH 7.4) for 1 h in an ice bath in the dark. Fixed specimens were rinsed in Milli-Q water (3 × 5 min) and dehydrated through successive baths of ethanol. Finally, samples were embedded into Spurr's resin (Science Services, Munich, Germany). After polymerization at 60 °C for 24h, semi-thin sections were cut to 800 nm thickness for quality control and then ultra-thin (ca. 70-80 nm) sections were cut for examination on a Leica EM UC6 ultramicrotome (Leica Microsystems, Germany) equipped with a 45º DiATOME diamond knife and floated on nickel grids (200 mesh).

Immunogold labeling was performed according to Skepper & Powell (2008) with minor modifications. Briefly, the grids were etched with drops of 4% sodium metaperiodate for 10

min to unmask antigenic sites on the surface of the section, rinsed three times on successive drops of MQ water, and placed on drops of 1% aqueous periodic acid for 10 min to remove eventual osmium tetroxide residue. Sections were then placed on a drop of blocking solution consisting of PBS 0.01 M, 0.01% Triton X-100, Glycine 20 mM, and 1% BSA for 10 min to reduce nonspecific binding of antibodies. The anti-DA antibody (abcam) was diluted 1:200 in blocking solution, and the sections were incubated with the primary antibody solution overnight at 4 °C in a moist chamber. After washing with blocking solution (6 × 5 min), the sections were incubated with the Goat anti-Rabbit IgG secondary antibody conjugated with 6-nm gold particles (abcam/ab41498) diluted 1:500 in blocking solution for 2 h at 28 °C, and consecutively rinsed in blocking solution and MQ water. Contrast reagents (e.g. uranyl acetate and lead citrate) were not applied to avoid masking the nanogold particles. Immunogold labeling experimental conditions, as well as antibody optimization-dilutions are shown in Table II. Finally, the samples were examined under a transmission electron microscope JEOL JEM 1400 operated at 120 kV on the imaging platform of Brest University. The autophagosomal structures identified in this work by means of MET were classified according to their morphology and stage of development in marine bivalve cells (Owen, 1972; Yurchenko & Kalachev, 2019; Picot *et al.*, 2019).

2.5. Statistical analysis

To determine significant differences in toxin burdens in the digestive gland of scallops collected in the different sampling sites, *a priori* Fligner-Killeen's and Shapiro–Wilk test were used to evaluate the heterogeneity of variances and normality of frequencies of the data, respectively (Hector, 2015); the assumptions were not met. Values of DA concentrations were analyzed using a Kruskal-Wallis Test, where "the sampling site" was fixed as factor. In case of significant differences, a *post hoc* pairwise Wilcoxon rank test with Benjamini & Hochberg (BH) p-value adjustment was used to detect differences among means. For IHC results, Chi-

square test (χ^2) were applied to assess statistically significant differences in the chromogenic anti-DA signal present in each tissue of the scallops. When needed, *a posteriori* Tukey HSD test were used to identify differences between means. All the statistical analyses were performed using command lines in the R language (R v. 4.0.2, R Core Team, 2017), and graphics were generated with the R package ggplot2 on the Rstudio programming interface. All values are expressed as mean ± standard error (SE). Differences were considered statistically significant at $\alpha = 0.05$ for all analyses (Hector, 2015).

3. Results

3.1. Domoic acid (DA) quantification

Significant differences in the amount of DA accumulated in the digestive gland (DG) of the scallops from the three sampling sites were found after toxin quantification analysis by HPLC-UV (Fig. 1). Highest burdens ($P < 0.05$) of toxin were recorded in animals from Concarneau (CN) (446.6 ± 101.3 mg DA kg^{-1}) followed by those from Camaret-sur-Mer (CM) (82.5 ± 4.9 mg DA kg^{-1}), while the significant lowest values were detected in the scallops from the Bay of Brest (BB) (1.6 ± 0.4 mg DA kg^{-1}).

3.2. Histology and immunohistochemistry (IHC)

The presence of DA was detected by IHC, as brown chromogenic signal, within the tissues of all contaminated scallops (Fig. 2, 3 and 4). The absence of non-specific background staining during IHC process was confirmed in control slides incubated with the secondary antibody but without the primary anti-DA antibody (Fig. 2 A-C, Fig. 3 C, D and Fig. 4 E-H). The DA brown chromogenic signal was observed mainly throughout the DG, and readily detected in highly contaminated scallops from CN and CM. The typical DA immuno-staining observed in the DG of scallops sampled at CN and CM is illustrated in Figures 2D-F. As shown in Fig. 2D, within the DG, the strongest immunoreactivity was observed in small (~1-2.5 µm) spherical inclusion bodies (IBs) distributed exclusively throughout the cytoplasm of the

digestive (absorptive) cells of the digestive diverticula, which trapped an intense chromogenic staining (Fig. 2E, F). The anti-DA chromogenic signal detected in the DG of scallops from CN and CM has the same sub-cellular localization although DA burdens were significantly different between scallops from the two locations.

The multichromic staining allowed to clearly identifying these IBs within the cytoplasm of the digestive cells (Fig. 2G). As observed in Fig. 2H and 2I, the IBs had a dark violet-magenta dye, indicating the presence of neutral carbohydrates and neutral glycoconjugates on their surface. The IBs did not acquire any coloration with the conventional H&E staining (Fig. 2L). No histopathological patterns were observed in the DG of the scallops, even for the highest toxin burdens (Fig. 2J, K). The overall histological evidence allowed to observe that the IBs with DA-immunoreactivity were found mainly in the digestive cells of the diverticula in stages of active digestion (Fig. 2F, H, I, K, L).

In the samples from significantly weakly-contaminated scallops from BB, a slight-blurred and not well-located DA-chromogenic signal was observed in the "breakdown" and "regenerating" digestive diverticula of the DG (Fig. 3A-B). Nonetheless, it was possible to localize a few IBs with immunoreactivity in the cytoplasm of the remaining digestive cells (Fig. 3B). The H&E staining also allowed corroborating the absence of histopathologies in the DG due to DA accumulation (Fig. 3E, F).

The DA-localization in the rest of the tissues was similar in all the scallops contaminated from ~2 up to ~750 mg DA kg^{-1} (Fig. 4). The DA-labeling was detected only in the mucus of the epithelia that lines the outer part of the stomach (Fig. 4A), in the globose cells embedded in the epithelium of the intestine (Fig. 4B), and in the globose cells of the spawning channels or gonadic ducts in the female (Fig. 4C) and male (Fig. 4D) gonads. No DA signal was found in any other tissues such as gills, mantle, labial palps, kidneys or adductor muscle. With the

multichromic staining, it was possible to corroborate the presence of a light-blue coloration corresponding to acid glycoconjugates in the globose cells with immunolabeling (Fig. 4I-L). As seen in Fig. 4M-P, no histopathologies were observed in any of the additional tissues analyzed in this work.

As shown in Table IV, DA staining coverage in the DG was the same ($P > 0.05$) for scallops from CN and CM, while the anti-DA chromogenic signal detected in the DG of the scallops collected at BB was significantly lower. On the other hand, the chromogenic signal detected in the rest of the tissues (stomach, intestine, ovary, and testicle) was not different ($P > 0.05$) between the strongly (CN and CM) and weakly (BB) contaminated scallops.

3.3. Immunoelectron microscopy

The IBs observed in the cytoplasm of the digestive cells in the diverticula of scallops with a dark-violet coloration by means of multichromic staining, and presenting a strong DA-immunostaining were analyzed by transmission electron microscopy (TEM) in order to decipher their cellular nature (Fig. 5). The diameter of these IBs ranged between 1-2.5 µm. Early single-membrane-bound IBs structures (Fig. 5A) were observed frequently in the apical and sub-apical regions of the digestive cells. Meanwhile late-developed structures with a double-membrane-bound and a halo (Fig. 5B) were observed mainly in the mid-basal region of the cytoplasm, and often clustered into groups of 3-6 vesicles that may be or not surrounded by a single-membrane (Fig. 5C) and fusing with the lysosomes of the cell (Fig 5D). The morphological observations by TEM described above allowed identifying these IBs as autophagic vesicles.

On a second hand, we coupled the use of the specific anti-DA antibody and a secondary antibody conjugated with gold nanoparticles to the TEM analyzes (immunogold labeling). As seen in Fig. 5A-D, no anti-DA signal was observed in any subcellular structure of the GD in

316 the slide incubated without anti-DA primary antibody. By means of the immunogold labeling,
317 DA-signal was found mostly in the undigested material attached to the inner side of the
318 membranes within early (Fig. 5E-F) and late-autophagosomes (Fig. 5G-H), while a slight
319 signal of gold-nanoparticles corresponding to the toxin was observed in the halo of
320 autophagosomes and in the cytoplasm of the digestive cells (Fig. 5E-H).

321 **4. Discussion**

322 In this work, for the first time, immunolabeling by IHC using photonic microscopy and
323 immunogold using TEM has been successfully used for the localization of DA at the
324 subcellular level in naturally contaminated marine mollusc tissues. The technique set up in the
325 present paper has been shown to work for the immunostaining of DA with high precision,
326 either in heavily contaminated (up to 750 mg DA kg^{-1} GD) or in weakly-contaminated
327 scallops (~1 mg DA kg^{-1} DG) without nonspecific labeling. Although other methods, such as
328 HPLC-UV/MS (Quilliam *et al.,* 1989) and ELISA (Litaker *et al.,* 2008), have been widely
329 used to quantify DA content in contaminated shellfish with a high-resolution power (0.1 – 1
330 µg DA g^{-1}), they do not allow the subcellular visualization of DA in the tissues, as opposed to
331 the immunolabeling methods developed in this study. Furthermore, this immunostaining
332 method has proven to be suitable to be coupled with TEM, allowing to pinpoint DA
333 localization.

334 Using a subcellular fractionation analysis on homogenized DA-contaminated digestive glands
335 of *P. maximus,* Mauriz & Blanco (2010) found that almost 90% of the toxin accumulated in
336 this organ was in soluble form in the cytoplasm of the cells, with a mostly homogeneous
337 distribution within the DG (Blanco *et al.* 2020). One mechanism that could influence high
338 accumulation and long retention of DA in this species could be its binding to high affinity
339 receptors, as those found in the razor clam *S. patula* (Trainer & Bill, 2004). Moreover, Mauriz

& Blanco (2010) concluded that the cause of the long DA-retention was not the binding of the toxin to some cellular component, but the lack of some efficient membrane transporters in the scallops. Our results cope with these findings, since most of the DA immune-signal was localized in the cytoplasm of the digestive cells of the digestive diverticula. Several digestive stages (holding, absorptive, digestion, advanced digestion, breakdown, and regeneration) have been described for the digestive diverticula of *P. maximus* (Mathers, 1976). In this work, the inclusion bodies (IBs) with anti-DA signal were observed mostly in the digestive cells of the diverticula in states of active digestion (absorption, digestion and advanced digestion). This is probably due to digestive cells predominate in these digestion stages and are responsible for the intracellular enzymatic digestion of the material ingested by pinocytosis (Beninger & Le Pennec, 2016). Free domoic acid in the cytoplasm was visualized by immunogold. Nonetheless, the evidence of this work suggests that a significant proportion of the toxin is not simply "free-dissolved" in the cytoplasm, but is enclosed in small (1-2.5 µm) membrane-bound vesicles, identified as autophagosomal structures by means of TEM, distributed throughout the cytoplasm of digestive cells in digestive condition.

Autophagy is a well-developed, highly regulated, and complex-dynamic system related to ingestion, storage and catabolic processes of intracellular digestion (Balbi *et al.,* 2018; Wang *et al.,* 2019; Zhao *et al.,* 2021). In bivalves, autophagy plays a key role in maintaining cell homeostasis (Carella *et al.,* 2015). This mechanism has been used as an indicator of cell injury in response to different stressors (Moore, 2004; Picot *et al.,* 2019), such as environmental changes (Moore, 2008), and the innate-immune response to pathogens (Canesi *et al.,* 2002; Moreau *et al.,* 2015; Canesi *et al.,* 2016; Balbi *et al.,* 2018) However, nothing is still known on the role of autophagy in ingestion, mobilization and excretion of phycotoxins in these organisms.

During autophagy, cytoplasmic components, either of exogenous (e.g. contaminants, and pathogens), or endogenous (macromolecules and organelles) origin are sequestered into spherical-shaped vesicles with double membrane layers called autophagosomes. Subsequently, they are delivered to lysosomes for degradation, where the outer membrane of the autophagosome fuses with a lysosome to form an autolysosome (Cuervo, 2004; Wang *et al.*, 2019). Finally, the hydrolases of the lysosome degrade the autophagosome-delivered contents and its inner membrane (Zhao *et al.*, 2021).

In samples of DA-contaminated scallops, mostly two types of membrane-bound autophagosomic vesicles were identified by transmission electron microscopy as part of this dynamic system. Early autophagosomes, which are usually involved in the ingestion and accumulation of exogenous materials, were present mainly in the apical region of the digestive cells; whereas in the mid- and basal regions of the cytoplasm we observed late-autophagosomes. These autophagosomes are involved in digestion and accumulation of undigested and indigestible residues, which may then be stored within the cell or eliminated (Owen, 1972; Zhao *et al.*, 2021). The transformation rate from early to late-autophagosomes is presumably dependent on the nature of the ingested material, and variations of this basic but highly-complex cycle probably depends on feeding rates, nature of the ingested food/substances, and the mode of release/excretion of the autophagosomic vesicles (Owen, 1972; Cuervo, 2004). The processing of autophagosomes by intracellular digestion could be a key to explain the long retention time of DA in the digestive cells of *P. maximus*. The toxin is probably normally ingested and accumulated in early autophagosomes, but cannot then be digested by the lysosomal machinery, thus remaining stored within autophagosomes as indigestible material in the cytoplasm of the cells. Moreover, it is difficult to know exactly how long it may take for the material present within autophagosomes to be excreted; since

388 some experiments suggest that it can go from a few minutes to indefinite periods of time
389 (Owen, 1972; Cuervo, 2004).

390 After DA injection in the adductor muscle, and subsequent transcriptomic analysis of the
391 digestive gland of *P. maximus*, Ventoso *et al.* (2021) found as well as an upregulation of
392 genes related to autophagy and vesicle-mediated transport. Even though these results were not
393 obtained under conditions of ingestion of the toxin through the filtration of toxic *Pseudo-*
394 *nitzschia* cells, these findings could also indicate that the formation of autophagosomic
395 structures could be part of explanation for DA long retention, blocking its digestion and
396 excretion.

397 In order to corroborate whether autophagy is the subcellular mechanism involved in the long
398 retention of DA in the DG of *P. maximus,* the next step would be to follow, by means of
399 digital image analysis, the evolution of the anti-DA chromogenic signal in the tissues in
400 parallel to the formation of autophagosomes with strong DA-immunoreactivity within the
401 digestive cells during the contamination and decontamination processes.

402 There is evidence of the profound interspecific differences in the retention and depuration of
403 DA in bivalves, even between pectinid species, like for example *P. maximus* and *A.*
404 *purpuratus*. While the former is capable of accumulating up to 3,000 mg DA kg^{-1} and retain it
405 for months or even years (Blanco *et al.,* 2006), *A. purpuratus* transfers almost all the DA
406 accumulated in the digestive gland to other organs (mainly the intestine and the gonad) within
407 a few days and then excrete the toxin into the environment (Álvarez *et al.*, 2020). Although
408 the physiological mechanisms enabling *A. purpuratus* to quickly depurate the DA are
409 unknown, Alvarez *et al.* (2020) hypothesized a two-compartment model, where the toxin
410 acquired by the DG is quickly transported to other organs. In *P. maximus,* we could
411 hypothesized that a significant part of DA accumulated stay in DG due to the absence of

412 specific transporter as proposed by Mauriz and Blanco (2020), and that, secondly, its its
413 detoxification be slower due to the formation of autophagosomes that retain the DA. Further
414 analyses, comparing these species, using histological, immunohistochemistry, as well as
415 molecular biology techniques appear necessary to confirm this hypothesis and to determine
416 whether autophagy appears in other slow-depurator shellfish species.

417 In the rest of the tissues of *P. maximus*, the IHC technique developed in this work revealed
418 specific toxin-immunoreactivity and thus DA-localization within the mucus, particularly in
419 the mucocytes of some epithelia such as the stomach and intestine, and in the mucocytes of
420 the gonad spawning-ducts. Mucus is composed of water, glycoproteins and mineral salts
421 (Davies & Hawkins, 1998), and is produced by almost all the epithelia of mollusks, playing
422 an essential role in several functions such as lubrication, nutrition, the first barrier against
423 environmental stress, and as an innate-immune barrier against pathogenic infections (Allam &
424 Pales Espinosa, 2015). Hence, complementary studies are necessary to determine if DA has
425 an affinity or is chemically-bounded to any of the components of mucus, and if the latter may
426 be involved in DA-depuration or retention in the scallops. This hypothesis is totally new,
427 since DA detection techniques in contaminated bivalve tissues had never allowed to localize
428 the toxin at the level of mucus or mucus-producing cells during a contamination and
429 decontamination scenario.

430 **5. Conclusions**

431 The DA-immunodetection methods proposed in this work by immunohistochemistry and
432 immunogold are innovative ways to visualize the phycotoxin DA in the tissues of the king
433 scallop *P. maximus*, and to decipher the subcellular mechanism involved in the retention of
434 this toxin in a marine bivalve. The results of this work show that, most of the DA is found in
435 the cytoplasm of digestive cells of *P. maximus*, as previously mentioned by Mauriz & Blanco

(2010). Notwithstanding, most part of DA-signal does not appear free in the cytoplasm, but mainly within autophagic structures as revealed by DA-immunostaining, suggesting that autophagic subcellular mechanisms could play a crucial role in the retention of the ASP toxin in the digestive cells of scallops. Furthermore, the role of mucus in the retention-depuration of DA in *P. maximus* must be investigated, since the toxin was only immunolocalized in the mucus of specific remaining tissues.

DA-immunodetection also provides a great tool to compare DA-localisation within species depurating at different speed over a contamination and decontamination period. The findings of this work constitute an important step forward in explaining the slow depuration of DA in *P. maximus*, and provide basic knowledge for the proposal of procedures to accelerate the depuration of the toxin in this species.

Acknowledgments

The authors are grateful to Aouregan Terre-Terrillon and Erwan Amice for the scallop sampling. We thank Nelly Le Goïc and Adeline Bidault (from IUEM-LEMAR, Brest) for their technical support. We also thank Amélie Derrien and Malwenn Lassudrie (Ifremer, Concarneau) for their valuable help with HPLC technique, as well as Philippe Elies (PIMM platform, UBO, Brest) for his assistance with transmission electron microscopy.

Conflict of interest

All authors approved the final version of this manuscript and declare no conflict of interest.

Funding

This work received financial support from the research project “MaSCoET” (Maintien du Stock de Coquillages en lien avec la problématique des Efflorescences Toxiques) financed by France Filière Pêche and Brest Métropole, and the project “CoDDA” (Contamination and Decontamination of Domoic Acid in marine bivalves) funded by ISblue under the academic

responsibility of JLGC, CF and HH. JLGC is recipient of a doctorate fellowship from CONACyT, Mexico (REF: 2019-000025-01EXTF-00067).

Data availability statement

The evidence and data that support the findings of this study are available from the corresponding author upon reasonable request.

Ethics statements

The adult scallops (*Pecten maximus*) were transported and handled according to the International Standards for the Care and Use of Laboratory Animals. The number of sampled organisms contemplated "the rule of maximizing information published and minimizing unnecessary studies". In this sense, 20 scallops were considered as the minimum number of organisms needed for this work.

Literature cited

Allam, B., & Pales Espinosa, E. (2016). Bivalve immunity and response to infections: Are we looking at the right place? *Fish & Shellfish Immunology*, 53, 4–12. https://doi.org/10.1016/j.fsi.2016.03.037

Álvarez, G., Rengel, J., Araya, M., Álvarez, F., Pino, R., Uribe, E., Díaz, P.A., Rossignoli, A.E., López-Rivera, A., & Blanco, J. (2020). Rapid Domoic Acid Depuration in the Scallop *Argopecten purpuratus* and Its Transfer from the Digestive Gland to Other Organs. *Toxins*, 12, 698. https://doi.org/10.3390/toxins12110698

Balbi, T., Cortese, K., Ciacci, C., Bellese, G., Vezzulli, L., Pruzzo, C., & Canesi, L. (2018). Autophagic processes in Mytilus galloprovincialis hemocytes: effects of *Vibrio tapetis*. *Fish & Shellfish Immunology*, 73, 66–74. https://doi.org/10.1016/j.fsi.2017.12.003

Basti, L., Hegaret, H., & Shumway, S.E. (2018). Harmful Algal Blooms and Shellfish. In Shumway, S.E., Burkholder, J.M., Morton, S.L., eds. Harmful Algal Blooms a Compendium Desk Reference, pp.135–191. John Wiley & Sons Inc., Hoboken, NJ.

Bates, S. S., Hubbard, K. A., Lundholm, N., Montresor, M., & Leaw, C. P. (2018). *Pseudo-nitzschia, Nitzschia*, and domoic acid: New research since 2011. *Harmful Algae*, http://dx.doi.org/10.1016/j.hal.2018.06.001

Blanco, J., Acosta, C. P., Mariño, C., Muñiz, S., Martín, H., Moroño, Á., Correa, J., Arévalo, F. & Salgado, C. (2006). Depuration of domoic acid from different body compartments of the king scallop *Pecten maximus* grown in raft culture and natural bed. *Aquatic Living Resources*, 19(3), 257–265. http://dx.doi.org/10.1051/alr:2006026

Blanco, J., Acosta, C., Bermúdez de la Puente, M., & Salgado, C. (2002). Depuration and anatomical distribution of the amnesic shellfish poisoning (ASP) toxin domoic acid in the king scallop *Pecten maximus*. *Aquatic Toxicology*, 60(1-2), 111–121. http://dx.doi.org/10.1016/s0166-445x(01)00274-0

Blanco, J., Mauríz, A. & Álvarez, G. (2020). Distribution of Domoic Acid in the Digestive Gland of the King Scallop *Pecten maximus*. *Toxins*, 12(371), 1-11. http://dx.doi.org/10.3390/toxins12060371

Bogan, Y.M., Harkin, A.L., Gillespie, J., Kennedy, D.J., Hess, P., & Slater, J.W. (2007). The influence of size on domoic acid concentration in king scallop, *Pecten maximus* (L.). *Harmful Algae*, 6, 15–28. https://doi.org/10.1016/j.hal.2006.05.005

Bresnan, E., Fryer, R. J., Fraser, S., Smith, N., Stobo, L., Brown, N., & Turrell, E. (2017). The relationship between *Pseudo-nitzschia* (Peragallo) and domoic acid in Scottish shellfish. *Harmful Algae*, 63, 193–202. https://doi.org/10.1016/j.hal.2017.01.004

Beninger, P. G., & Le Pennec, M. (2016). Structure and function in scallops. In S. E. Shumway, & G. J. Parsons (Eds.), Scallops: Biology, ecology, aquaculture, and fisheries (pp. 85–159). Elsevier.

Canesi, L., Ciacci, C., & Balbi, T. (2016). Invertebrate Models for Investigating the Impact of Nanomaterials on Innate Immunity: The Example of the Marine Mussel *Mytilus* spp. *Current Bionanotechnology*, 2(2), 77-83. https://doi.org/10.2174/2213529402666160601102529

Canesi, L., Gallo, G., Gavioli, M., & Pruzzo, C. (2002). Bacteria-hemocyte interactions and phagocytosis in marine bivalves. *Microscopy Research and Technique*, 57(6), 469–476. https://doi.org/10.1002/jemt.10100

516 Carella, F., Feist, S., Bignell, J., & De Vico, G. (2015). Comparative pathology in bivalves:
517 aetiological agents and disease processes. *Journal of Invertebrate Pathology*, 131, 107–120.
518 https://doi.org/10.1016/j.jip.2015.07.012

519 Costa, P. & Costa, M.H. (2012). Development and application of a novel histological
520 multichrome technique for clam histopathology. *Journal of Invertebrate Pathology*, 110, 411-
521 414. http://dx.doi.org/10.1016/j.jip.2012.04.013

522 Cuervo, A. M. (2004). Autophagy: Many paths to the same end. *Molecular and Cellular*
523 *Biochemistry*, 263(1/2), 55–72. https://doi.org/10.1023/b:mcbi.0000041848.57020.57

524 Davies, M.S. & Hawkins, S.J. (1998). Mucus from Marine Molluscs. pp. 1–71. In: Blaxter
525 J.H.S., Southward A.J., & Tyler P.A. (eds), Advances in Marine Biology, Academic Press.

526 Delegrange, A., Lefebvre, A., Gohin, F., Courcot, L., & Vincent, D. (2018). *Pseudo-nitzschia*
527 *sp.* diversity and seasonality in the southern North Sea, domoic acid levels and associated
528 phytoplankton communities. *Estuarine, Coastal and Shelf Science*, 214, 194–206.
529 https://doi.org/10.1016/j.ecss.2018.09.030

530 Douglas, D. J., Kenchington, E. R., Bird, C. J., Pocklington, R., Bradford, B., & Silvert, W.
531 (1997). Accumulation of domoic acid by the sea scallop (*Placopecten magellanicus*) fed
532 cultured cells of toxic *Pseudo-nitzschia multiseries*. *Canadian Journal of Fisheries and*
533 *Aquatic Sciences*, 54(4), 907–913. https://doi.org/10.1139/f96-333

534 EFSA. (2009). Panel on Contaminants in the Food Chain. Scientific Opinion of the Panel on
535 Contaminants in the Food Chain on a request from the European Commission on marine
536 biotoxins in shellfish—Domoic acid. EFSA J., 1181, 1–61.

537 FAO. 2020. The State of World Fisheries and Aquaculture 2020. Sustainability in action.
538 Rome. https://doi.org/10.4060/ca9229en

539 Ha, D. V., Takata, Y., Sato, S., Fukuyo, Y., & Kodama, M. (2006). Domoic acid in a bivalve
540 *Spondylus cruentusin* Nha Trang Bay, Khanh Hoa Province, Vietnam. *Coastal Marine*
541 *Science*, 30(1), 130–132.

542 Hallegraeff, G.M. (2017). Marine phycotoxins and seafood safety. In: Witczak, A., Sikorski,
543 Z.E. (Eds.), Toxins and Other Harmful Compounds in Foods. CRC Press, Taylor & Francis
544 Group, Boca Raton, Florida, pp. 63–84.

545 Hector, A. (2015). The new statistics with R: an introduction for biologists (1st ed.). New
546 York, Oxford University Press.

547 Horner, R.A., Kusske, M.B., Moynihan, B.P., Skinner, R.N. & Wekell, J.C. (1993). Retention
548 of Domoic Acid by Pacific Razor Clams, *Siliqua patula* (Dixon, 1789): Preliminary Study.
549 *Journal of Shellfish Research*, 12, 451-456.

550 Jones, T. O., Whyte, J. N. C., Ginther, N. G., Townsend, L. D., & Iwama, G. K. (1995).
551 Haemocyte changes in the pacific oyster, *Crassostrea gigas*, caused by exposure to domoic
552 acid in the diatom *Pseudonitzschia pungens f. multiseries. Toxicon,* 33(3), 347–353.
553 https://doi.org/10.1016/0041-0101(94)00170-

554 Kim, Y., Ashton-Alcox, K.A. & Powell, E.N. (2006). Histological Techniques for Marine
555 Bivalve Molluscs: update. NOAA Technical Memorandum NOS NCCOS 27, Maryland.

556 Lefebvre, K. A., & Robertson, A. (2010). Domoic acid and human exposure risks: A review.
557 *Toxicon*, 56(2), 218–230. http://dx.doi.org/10.1016/j.toxicon.2009.05

558 Lelong, A., Hégaret, H., Soudant, P., & Bates, S. S. (2012). *Pseudo-nitzschia*
559 (Bacillariophyceae) species, domoic acid and amnesic shellfish poisoning: revisiting previous
560 paradigms. *Phycologia*, 51(2), 168–216. http://dx.doi.org/10.2216/11-37.1

561 Litaker, R. W., Stewart, T. N., Eberhart, B.-T. L., Wekell, J. C., Trainer, V. L., Kudela, R. M.,
562 Miller, P.E., Roberts, A., Hertz, C., Johnson, T.A., Frankfurter, G., Smith, G.J., Schnetzer, A.,
563 Schumacker, J., Bastian, J.L., Odell, A., Gentien, P., Le Gal, D., Hardison, D.R., & Tester, P.
564 A. (2008). Rapid Enzyme-linked Immunosorbent Assay for Detection of the Algal Toxin
565 Domoic Acid. *Journal of Shellfish Research*, 27(5), 1301–1310. https://doi.org/10.2983/0730-
566 8000-27.5.1301

567 Lundholm, N., Churro, C., Fraga, S., Hoppenrath, M., Iwataki, M., Larsen, J., Mertens, K.,
568 Moestrup, Ø., & Zingone, A. (Eds) (2009 onwards). IOC-UNESCO Taxonomic Reference
569 List of Harmful Micro Algae. Accessed at https://www.marinespecies.org/hab on 2022-02-20.
570 https://doi.org/10.14284/362

571 Mackenzie, A.L., White, D.A., Sim, P.G., & Holland, A.J. (1993). Domoic acid and the New
572 Zealand greenshell mussel (*Perna canaliculus*). In: Smayda, T.J., Shimizu, Y. (Eds.), Toxic
573 Phytoplankton Blooms in the Sea. Elsevier Science Publishers, pp. 607–612.

574 Mafra, L. L., Bricelj, V. M., & Fennel, K. (2010). Domoic acid uptake and elimination
575 kinetics in oysters and mussels in relation to body size and anatomical distribution of toxin.
576 *Aquatic Toxicology*, 100(1), 17–29. https://doi.org/10.1016/j.aquatox.2010.07.0

577 Mathers, N. F. (1976). The effects of tidal currents on the rhythm of feeding and digestion in
578 *Pecten maximus* L. Journal of Experimental Marine Biology and Ecology, 24(3), 271-283.
579 https://doi.org/10.1016/0022-0981(76)90059-9

580 Mauriz, A., & Blanco, J. (2010). Distribution and linkage of domoic acid (amnesic shellfish
581 poisoning toxins) in subcellular fractions of the digestive gland of the scallop *Pecten*
582 *maximus*. *Toxicon*, 55(2-3), 606–611. https://doi.org/10.1016/j.toxicon.2009.10.

583 Moore, M. N. (2004). Diet restriction induced autophagy: A lysosomal protective system
584 against oxidative- and pollutant-stress and cell injury. *Marine Environmental Research*, 58(2-
585 5), 603–607. https://doi.org/10.1016/j.marenvres.2004.03

586 Moore, M. N. (2008). Autophagy as a second level protective process in conferring resistance
587 to environmentally-induced oxidative stress. *Autophagy*, 4(2), 254–256.
588 https://doi.org/10.4161/auto.5528

589 Moreau, P., Moreau, K., Segarra, A., Tourbiez, D., Travers, M.-A., Rubinsztein, D. &
590 Renault, T. (2015). Autophagy plays an important role in protecting Pacific oysters from
591 OsHV-1 and *Vibrio aestuarianus* infections. *Autophagy*, 11, 516–526.
592 https://doi.org/10.1080/15548627.2015.1017188

593 Novaczek, I., Madhyastha, M. S., Ablett, R. F., Donald, A., Johnson, G., Nijjar, M. S., &
594 Sims, D. E. (1992). Depuration of Domoic Acid from Live Blue Mussels (*Mytilus edulis*).
595 *Canadian Journal of Fisheries and Aquatic Sciences*, 49(2), 312–318.
596 https://doi.org/10.1139/f92-035

597 Owen, G. (1972). Lysosomes, peroxisomes and bivalves. Science Progress, 60(239), 299–
598 318.

599 Picot, S., Morga, B., Faury, N., Chollet, B., Dégremont, L., Travers, M.-A., Renault, T. &
600 Arzul, I. (2019). A study of autophagy in hemocytes of the Pacific oyster, *Crassostrea gigas*.
601 *Autophagy*, 1–9. https://doi.org/10.1080/15548627.2019.1596

602 Quilliam, M. A., Sim, P. G., McCulloch, A. W., & McInnes, A. G. (1989). High-Performance
603 Liquid Chromatography of Domoic Acid, a Marine Neurotoxin, with Application to Shellfish

and Plankton. *International Journal of Environmental Analytical Chemistry*, 36(3), 139–154. https://doi.org/10.1080/03067318908026867

R Core Team (2018). R: A language and environment for statistical computing. R Foundation for Statistical Computing,Vienna, Austria. URL https://www.R-project.org/.

Skepper, J.N. & Powell, J.M. (2008). Immunogold Staining of Epoxy Resin Sections for Transmission Electron Microscopy (TEM). *CSH Protocols*, 3(6), 1-4. http://dx.doi.org/10.1101/pdb.prot5015

Trainer, V. L., Bates, S. S., Lundholm, N., Thessen, A. E., Cochlan, W. P., Adams, N. G., & Trick, C. G. (2012). *Pseudo-nitzschia* physiological ecology, phylogeny, toxicity, monitoring and impacts on ecosystem health. *Harmful Algae*, 14, 271–300. http://dx.doi.org/doi:10.1016/j.hal.2011.10.025

Trainer, V.L. & Bill, B.D. (2004). Characterization of a domoic acid binding site from Pacific razor clam. *Aquatic Toxicology*, 69, 125–132. http://dx.doi.org/10.1016/j.aquatox.2004.04.012

Thomas, K. M., LeBlanc, D. M., & Quilliam, M. A. (1998). The 112th AOAC International Annual Meeting and Exposition, AOAC, Montreal.

Ventoso, P., Pazos, A.J., Blanco, J., Pérez-Parallé, M.L., Triviño, J.C., & Sánchez, J.L. (2021). Transcriptional Response in the Digestive Gland of the King Scallop (*Pecten maximus*) After the Injection of Domoic Acid. *Toxins*, 13, 339. https://doi.org/10.3390/toxins13050339

Wang, L., Ye, X., & Zhao, T. (2019). The physiological roles of autophagy in the mammalian life cycle. *Biological Reviews*, 94, 503–516. https://doi.org/10.1111/brv.12464

Wohlgeschaffen, G. D., Mann, K. H., Subba Rao, D. V., & Pocklington, R. (1992). Dynamics of the phycotoxin domoic acid: accumulation and excretion in two commercially important bivalves. *Journal of Applied Phycology*, 4(4), 297–310. https://doi.org/10.1007/bf02185786

Yurchenko, O., & Kalachev, A. (2019). Morphology of nutrient storage cells in the gonadal area of the Pacific oyster, *Crassostrea gigas* (Thunberg, 1793). *Tissue Cell* 56, 7–13. https://doi.org/10.1016/j.tice.2018.11.004

632 Zabaglo, K., Chrapusta, E., Bober, B., Kaminski, A., Adamski, M., & Bialczyk, J. (2016).
633 Environmental roles and biological activity of domoic acid: A review. *Algal Research*, 13,
634 94–101. http://dx.doi.org/10.1016/j.algal.2015.11.020

635 Zaman, L., Arakawa, O., Shimosu, A., Onoue, Y., Nishio, S., Shida, Y., & Noguchi, T.
636 (1997). Two new isomers of domoic acid from a red alga, Chondria armata. Toxicon, 35(2),
637 205-212. https://doi.org/10.1016/S0041-0101(96)00123-7

638 Zhao, Y. G., Codogno, P., & Zhang, H. (2021). Machinery, regulation and pathophysiological
639 implications of autophagosome maturation. *Nature Reviews Molecular Cell Biology*.
640 http://dx.doi.org/10.1038/s41580-021-00392-4

Table I. Full stepwise sequence of the immunohistochemical staining method.

Step	Reagent/Solution	Duration	Temperature
Tissue processing			
Fixation	Davidson solution	24 to 48 h	~ 4 °C
Preservation	Ethanol 70%	Days/ months	~ 4 °C
Dehydration	Ethanol 80%, 95% and 100%	8 × 1 h	~ 20 °C
Clarifying	Claral	2 × 1 h	~ 20 °C
Impregnation	Paraffin	Overnight	~ 60 °C
Staining			
Deparaffinization	Claral	2 × 3 min	~ 20 °C
Hydration	Ethanol 100%, 95% and 80%	5 × 3 min	~ 20 °C
Antigen retrieval	Universal HIER reagent 1×	3 min	~ 120 °C
Wash	Washing buffer[a]	3 × 5 min	~ 20 °C
Peroxidase quenching	Blocking peroxidase solution	2 h	~ 20 °C
Wash	Washing buffer	2 × 5 min	~ 20 °C
1st immune-staining	Primary Ab anti-DA	Overnight	~ 4 °C
Wash	Washing buffer	2 × 5 min	~ 20 °C
2nd immune-staining	Secondary Ab HRP conjugated	1 h	~ 37 °C
Wash	Washing buffer	2 × 5 min	~ 20 °C
Revelation	DAB+ substrate	10 min	~ 20 °C
Wash	Washing buffer	2 × 5 min	~ 20 °C
Counterstaining	Hematoxylin	1 min	~ 20 °C
Rinse	Tap water	A few dips	~ 20 °C

[a]TBS is recommended over PBS in washing buffer to get a cleaner background. 0.025% Triton X-100 in the TBS reduces surface tension, allowing reagents to cover the tissue section easily.
Ab = antibody

Table II. Antibody (Ab) optimization and immunohistochemical experimental conditions.

Conditions	Concentrations		Antigen retrieval[a]	Peroxidase Quenching[b]
	Primary Ab Anti-DA	*Secondary Ab* HRP/nanogold conjugated		
	IHC			
Negative control	Without	1: 10,000	Yes	Yes
Treated	1:1,000	1: 10,000	Yes	Yes
	Immunogold			
Negative control	Without	1: 500	No	No
Treated	1:200	1: 500	No	No

[a]Antigen retrieval allows to break potential methylene bridges formed during formalin-fixation and expose antigenic sites to allow the antibodies epitope to bind.
[b]Endogenous peroxidase blocking is necessary to avoid non-specific staining.

652 **Table III.** Semi-quantitative scale categorizing the intensity of chromogenic anti-DA signal
653 observed on the IHC slides.

Level intensity	Occurrence of the chromogenic anti-DA staining in the examined tissue area
0	Absence
0.5	Very low (<5 occurrence/presence in all fields at magnification 10×)
1	Low (>5 occurrence/presence in all fields at magnification 10×)
1.5	Moderate (presence in all fields at magnification 20×/ covering about one tenth of the tissue area)
2	High (presence in all fields at magnification 40×/ covering about one fifth of the tissue area)
2.5	Very high (presence in all fields at magnification 60×/ covering about one-third or above of the tissue area)

654

655 **Table IV.** Comparison of IHC staining intensity of DA in the tissues of the scallops *P.*
656 *maximus* naturally contaminated and collected at three sites (CN = Concarneau [n = 6], BB =
657 Bay of Brest [n = 7], and CM = Camaret-sur-mer [n = 7]) of the northwest coast of France
658 between 2019 and 2021. NA: not available (not enough data), "—": no chromogenic anti-DA
659 staining.

Tissue	Sampling site			Statistical analysis	
	CN	BB	CM	χ^2, *n*	*p*
Digestive gland	2.4 ± 0.08^a	0.57 ± 0.13^b	2.4 ± 0.09^a	20.4, 20	<0.05
Stomach	1.2 ± 0.11^a	0.93 ± 0.14^a	1.3 ± 0.1^a	5.9, 20	>0.05
Intestine	1.3 ± 0.1^a	1.07 ± 0.17^a	1.3 ± 0.1^a	4.3, 20	>0.05
Ovary	1.2 ± 0.1^a	0.93 ± 0.13^a	1.3 ± 0.1^a	5.8, 20	>0.05
Testicle	1.1 ± 0.09^a	1 ± 0.15^a	1.4 ± 0.09^a	4.2, 20	>0.05
Gills	—	—	—	NA	
Adductor muscle	—	—	—	NA	
Mantle	—	—	—	NA	
Labial palps	—	—	—	NA	

660 Data (mean ± SE) were analyzed according to the sampling sites (three levels) in a Chi-square
661 test (χ^2). The χ^2 test statistic and sample size (*n*) are reported. Different superscript letters
662 denote statistically significant differences at $p < 0.05$.

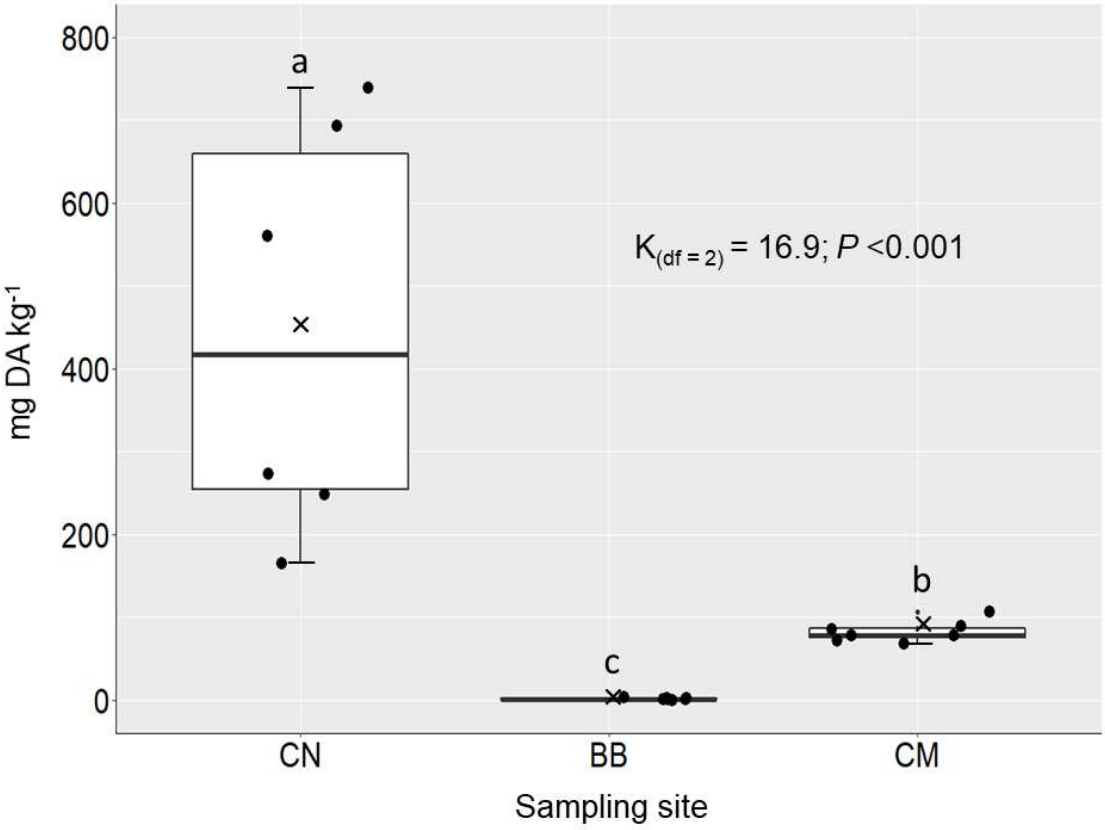

Figure 1. DA concentrations in the digestive gland of the scallops *P. maximus* naturally contaminated during outbreaks of the toxic *Pseudo-nitzschia* spp. and collected at three sites (CN = Concarneau [n = 6], BB = Bay of Brest [n = 7], and CM = Camaret-sur-mer [n = 7]) of the northwest coast of France between 2019 and 2021. The upper and lower limits of the boxes are the quartiles, the middle horizontal line is the median, the extremes of the vertical lines are the upper and lower limits of the observations, the dots are the individual observations, and the crosses are the means. Data were analyzed using the sampling sites (three levels) as independent variables in a Kruskal-Wallis Test. The K-test statistic and degrees of freedom (df) are reported. Different superscript letters denote statistically significant differences between groups of scallops. The level of statistical significance was set at $\alpha = 0.05$.

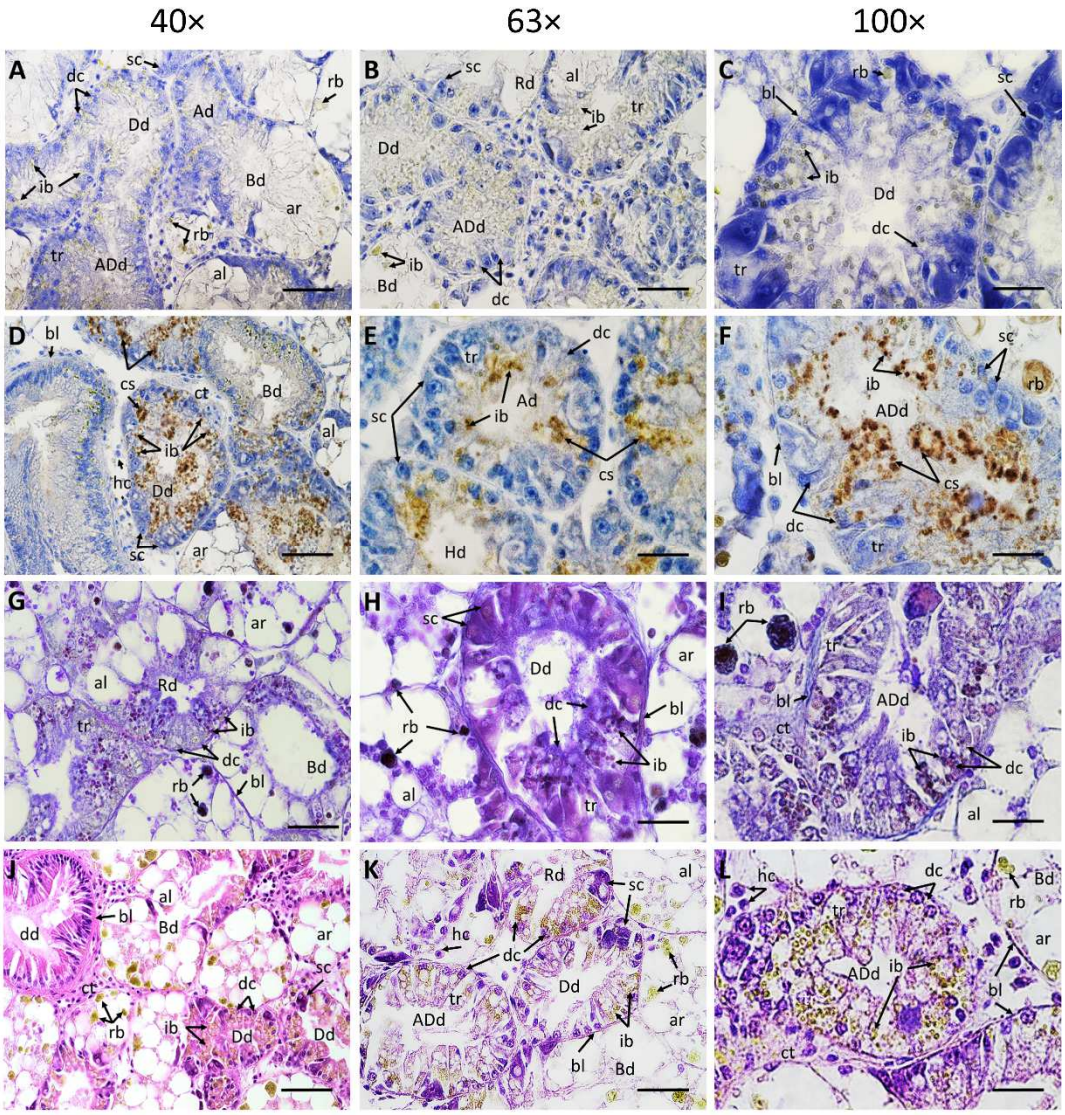

Figure 2. Microphotographs of digestive glands of scallops *P. maximus* naturally highly contaminated (~60 to 750 mg DA kg^{-1}) collected at Camaret-sur-mer (n = 7) and Concarneau (n = 6) in the northwest coast of France between 2019 and 2021during outbreaks of the toxic *Pseudo-nitzschia* spp. (A-C) negative controls of the IHC staining incubated with the secondary antibody but without the primary anti-DA antibody (1: 10,000 and 1: 0, respectively) ; (D-F) specific anti-DA immunohistochemical (IHC) staining incubated with the primary and secondary antibodies (1: 1,000 and 1: 10,000, respectively); (G-I) multichromic histochemical staining for the demonstration of neutral carbohydrates (violet-magenta dyes), acid glycoconjugates (blue hues), and proteins (yellowish tones); (J-L) conventional histological Hematoxylin-Eosin staining. Ad = digestive diverticulum in absorptive condition, ADd = digestive diverticulum in advanced digestive condition, al = adipocyte-like digestive cell, ar = acinar region, Bd = digestive diverticulum undergoing breakdown, bl = basal lamina, cs = positive anti-DA chromogenic signal, ct = connective tissue, dc = digestive cells, Dd = digestive diverticulum in digestive condition, dd = digestive duct, hc = hemocytes, Hd = digestive diverticulum in holding condition, ib = inclusion bodies, rb = residual bodies, Rd = diverticulum showing regeneration, sc = secretory cells, tr = tubular region. Scale bar: 40× = 50 µm, 63× = 30 µm, 100× = 10 µm.

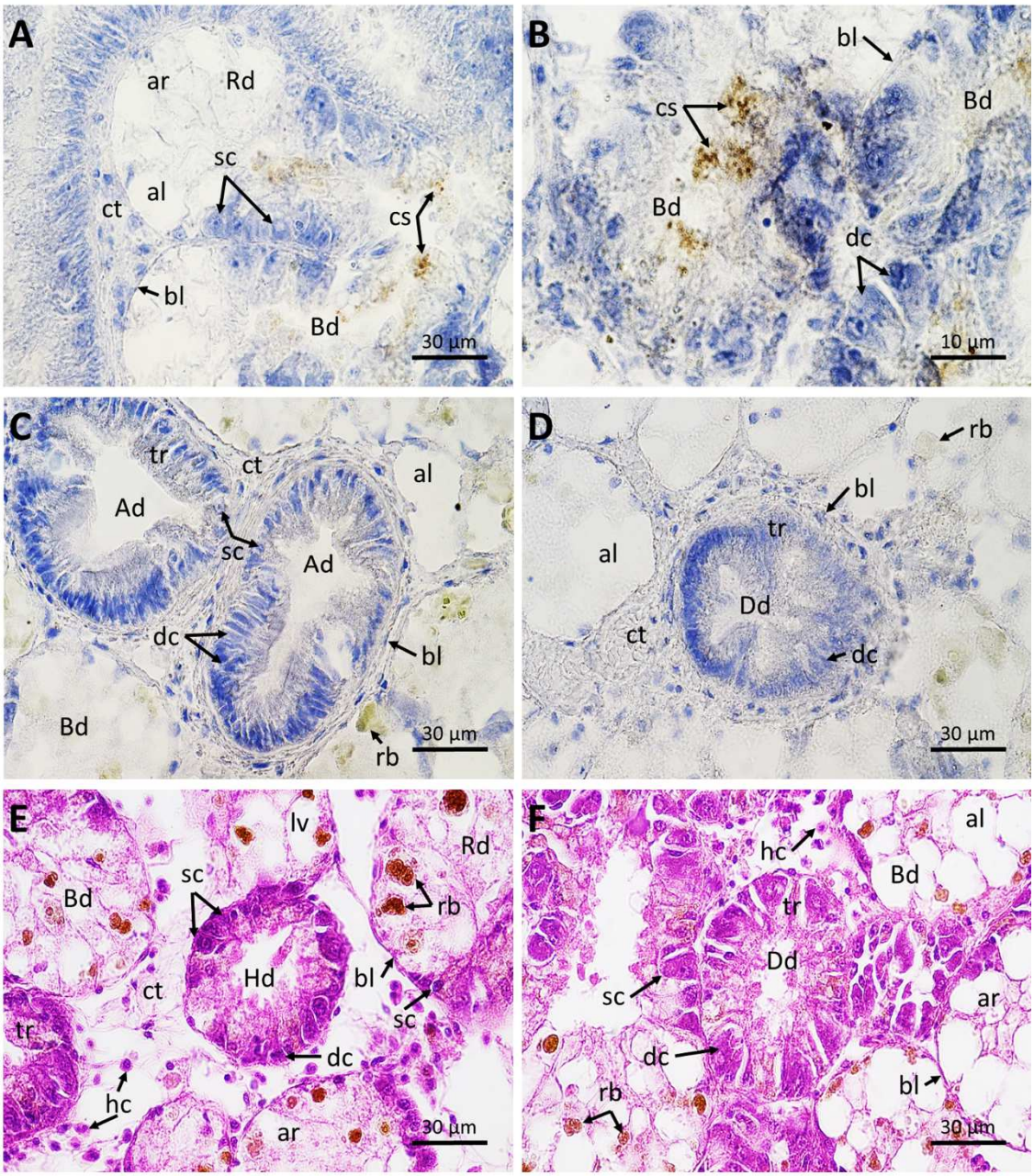

693

694 **Figure 3.** Microphotographs of digestive glands of scallops *P. maximus* naturally low
695 contaminated with ~2 mg DA kg^{-1} collected at the Bay of Brest (n = 7) on the northwest coast
696 of France in December 2020. (A-B) specific anti-DA immunohistochemical (IHC) staining
697 incubated with the primary and secondary antibodies (1: 1,000 and 1: 10,000, respectively);
698 (C-D) negative controls of the IHC staining incubated with the secondary antibody but
699 without the primary anti-DA antibody (1: 10,000 and 1: 0, respectively); (E-F) conventional
700 histological Hematoxylin-Eosin staining. Ad = digestive diverticulum in absorptive condition,
701 al = adipocyte-like digestive cell, ar = ascinar region, Bd = digestive diverticulum
702 undergoing breakdown, bl = basal lamina, cs = positive anti-DA chromogenic signal, ct =
703 connective tissue, dc = digestive cells, Dd = digestive diverticulum in digestive condition, hc
704 = hemocytes, Hd = digestive diverticulum in holding condition, rb = residual bodies, Rd =
705 diverticulum showing regeneration, sc = secretory cells, tb = tubular region.

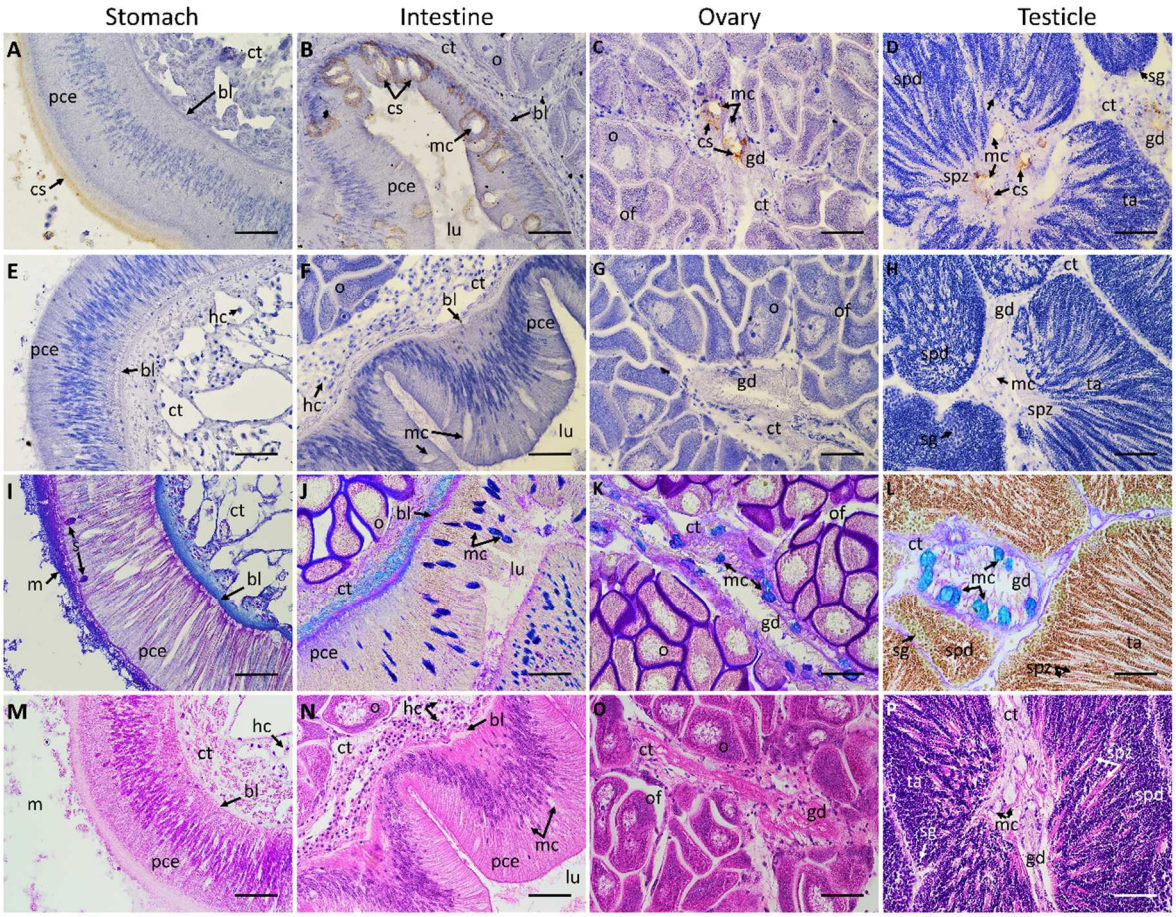

706

707 **Figure 4.** Microphotographs of the rest of the tissues of scallops *P. maximus* naturally
708 contaminated between ~2 and 750 mg DA kg^{-1} collected at three sites (Concarneau [n = 6],
709 Bay of Brest [n = 7], and Camaret-sur-mer [n = 7]) of the northwest coast of France between
710 2019 and 2021. (A-D) Specific anti-DA immunohistochemical (IHC) staining incubated with
711 the primary and secondary antibodies (1: 1,000 and 1: 10,000, respectively); (E-H) negative
712 controls of the IHC staining incubated with the secondary antibody but without the primary
713 anti-DA antibody (1: 10,000 and 1: 0, respectively); (I-L) multichromic histochemical
714 staining for the demonstration of neutral carbohydrates (violet-magenta dyes), acid
715 glycoconjugates (blue hues), and proteins (yellowish tones); (M-P) conventional histological
716 Hematoxylin-Eosin staining. bl = basal lamina, cs = positive anti-DA chromogenic signal, ct
717 = connective tissue, gd = gonadic duct, hc = hemocytes, lu = lumen, m = mucus, mc =
718 mucocyte, o = oocyte, of = ovarian follicle, pce = pseudostratified columnar epithelium, sg =
719 spermatogonia, spd = spermatids, spz = spermatozoa, ta = testicular acinus. Scale bar: 40× =
720 50 µm.

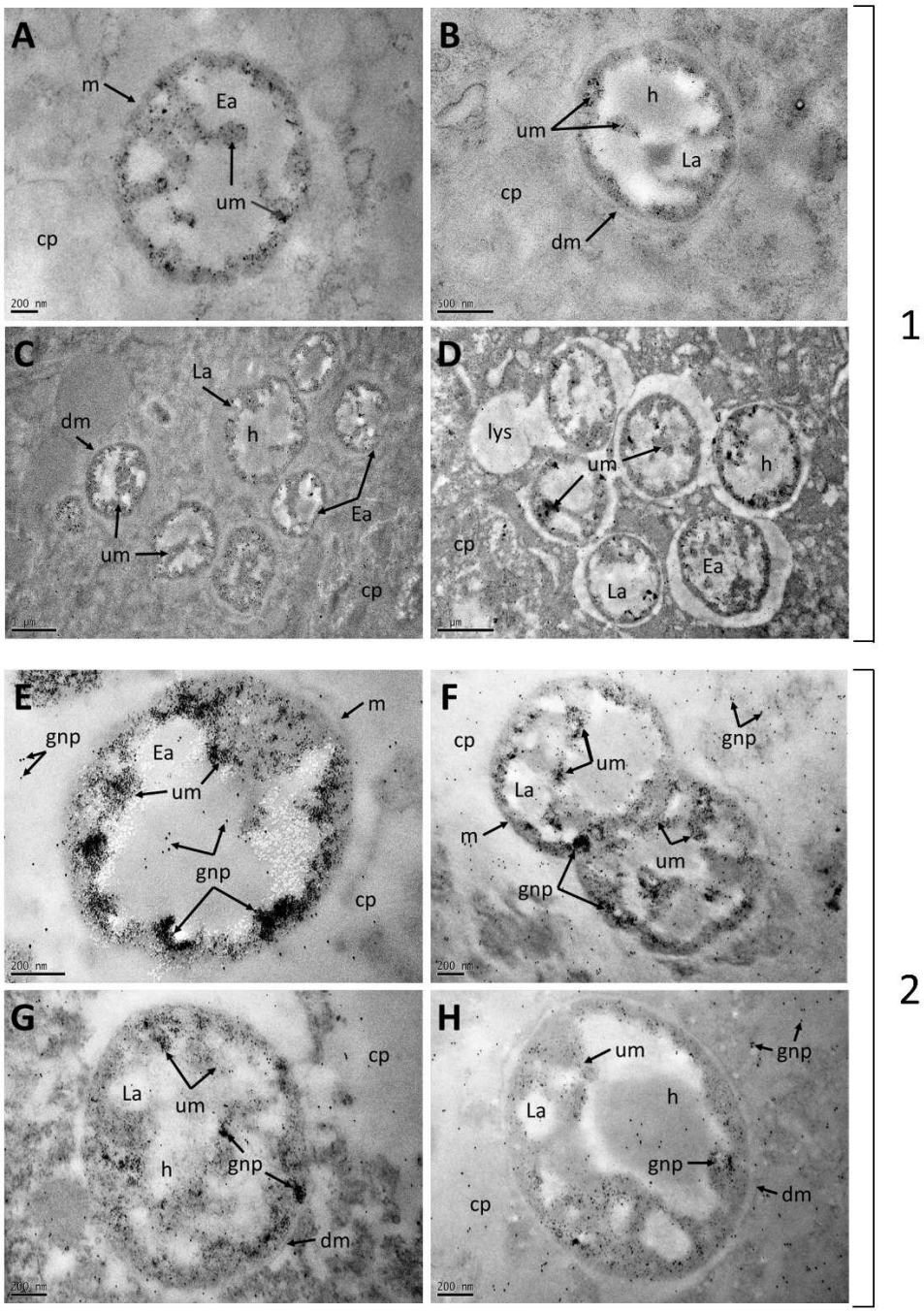

Figure 5. Electronmicrographs of ultrathin sections (70-80 nm) across the digestive glands of scallops *P. maximus* naturally contaminated (~75 mg DA kg^{-1}) during outbreaks of the toxic *Pseudo-nitzschia* spp. and collected in Camaret-sur-mer (n = 7) on the northwest coast of France in 2021. Detection of autophagic structures with positive DA immune-signal within digestive cells was possible by means of transmission electron microscopy (TEM). (1A-D) Negative controls of the immunogold labeling incubated with the secondary antibody but without the primary anti-DA antibody (1: 200 and 1: 0, respectively); (2E-H) Specific anti-DA immunogold labeling incubated with the primary anti-DA antibody and the secondary antibodies conjugated with 6-nm gold nanoparticles (1: 200 and 1: 500, respectively). cp = cytoplasm, dm = double-membrane-bound, Ea = early autophagosomes, gnp = gold nanoparticles, h = halo, La = late autophagosomes, lys = lysosomes, m = single-membrane-bound, um = undigested material.